Effect of Late-stage Therapy on Disease Progression in AAV-mediated Rescue of Photoreceptor Cells in the Retinoschisin-deficient Mouse

Andreas Janssen[1], Seok H Min[2], Laurie L Molday[3,4], Naoyuki Tanimoto[5], Mathias W Seeliger[5], William W Hauswirth[2,6,7], Robert S Molday[3,4] and Bernhard HF Weber[1]

[1]Institute of Human Genetics, University of Regensburg, Regensburg, Germany; [2]Department of Ophthalmology, University of Florida College of Medicine, Gainesville, Florida, USA; [3]Department of Biochemistry and Molecular Biology, University of British Columbia, Vancouver, British Columbia, Canada; [4]Department of Ophthalmology, Centre for Macular Research, University of British Columbia, Vancouver, British Columbia, Canada; [5]Ocular Neurodegeneration Research Group, Centre for Ophthalmology, Institute for Ophthalmic Research, University of Tuebingen, Tuebingen, Germany; [6]Department of Molecular Genetics and Microbiology, University of Florida College of Medicine, Gainesville, Florida, USA; [7]Gene Therapy Center, University of Florida College of Medicine, Gainesville, Florida, USA

Proof-of-concept for a successful adeno-associated virus serotype 5 (AAV5)-mediated gene therapy in X-linked juvenile retinoschisis (XLRS) has been demonstrated in an established mouse model for this condition. The initial studies concentrated on early time-points of treatment. In this study, we aimed to explore the consequences of single subretinal injections administered at various stages of more advanced disease. By electroretinogram (ERG), functional improvement in treated versus untreated eyes is found to be significant in retinoschisin-deficient mice injected at the time-points of 15 days (P15), 1 month (PM1), and 2 months (PM2) after birth. In mice treated at 7 months after birth (PM7), an age previously shown to exhibit advanced retinal disease, ERG responses reveal no beneficial effects of vector treatment. Generally, functional rescue is paralleled by sustained retinoschisin expression and significant photoreceptor survival relative to untreated eyes. Quantitative measures of photoreceptors and peanut agglutinin–labeled ribbon synapses demonstrate rescue effects even in mice injected as late as PM7. Taken together, AAV5-mediated gene replacement is beneficial in slowing disease progression in murine XLRS. In addition, we show the effectiveness of rescue efforts even if treatment is delayed until advanced signs of disease have developed. Human XLRS patients might benefit from these findings, which suggest that the effectiveness of treatment appears not to be restricted to the early stages of the disease, and that treatment may prove to be valuable even when administered at more advanced stages.

Received 16 October 2007; accepted 27 February 2008; published online 25 March 2008. doi:10.1038/mt.2008.57

INTRODUCTION

X-linked juvenile retinoschisis (XLRS) (OMIM #312700) was first described over 100 years ago[1] and, since then, it is known to be one of the more frequent hereditary retinal disorders affecting macular function in individuals of the male gender.[2] A hallmark of the disease is the localized splitting of the central retina. In most patients, visual acuity is reduced to 20/100 although this can vary greatly.[3,4] Thus far, treatment of XLRS has been limited to the prescription of low-vision aids. Surgical interventions benefit the patient only in rare cases.

An important functional test for XLRS is the full-field electroretinogram (ERG). Typically, a bright flash of light elicits a so-called negative response from the diseased retina, in which the a-wave is relatively preserved while the b-wave is nearly absent as compared to findings in a normal eye. The origin of this abnormality resides in the ON- and OFF-pathways at the level of the bipolar cells,[5] pointing to an important structural locus of disease pathology.

RS1 is the causative gene associated with XLRS and encodes a retina-specific 24 kd protein, named retinoschisin.[6] It is secreted mainly from photoreceptors as a disulfide-linked homo-oligomeric complex that is primarily localized to the outer surface of the inner segments of cones and rods but is also seen in the outer nuclear layer (ONL) and outer plexiform layer and in the bipolar cells of the inner nuclear layer (INL).[7–11] The mature protein consists almost exclusively of a discoidin domain,[12] a highly conserved module that likely mediates cell–cell interaction.[13,14]

The spectrum of *RS1* mutations comprises mostly missense mutations, followed by frame shift and nonsense mutations, as well as those probably resulting in a deficiency of functional protein. Disease-linked missense mutations have been shown to lead to misfolded, aggregated proteins that are mostly retained in the endoplasmic reticulum.[9,15] Together, these findings suggest that lack of functional retinoschisin underlies disease pathology. This raises

The first three authors contributed equally to this work.

Correspondence: *Bernhard H.F. Weber, Institute of Human Genetics, Franz-Josef-Strauss-Allee 11, University of Regensburg,D-93053 Regensburg, Germany. E-mail: bweb@klinik.uni-regensburg.de*

the possibility that replacement of the missing protein may be beneficial to patients regardless of the specific type of *RS1* mutation.

We[16] as well as others[17] have provided proof-of-concept for gene replacement in XLRS by demonstrating that intraocular adeno-associated virus (AAV) delivery of retinoschisin results in a significant recovery of retinal structure and function.[17,18] In our study, a subretinal injection of an AAV serotype 5 vector containing the human *RS1* gene under the control of the mouse opsin promoter (AAV5-mOPs-*RS1*) was administered at postnatal day 15 (ref. 16). This has led to a significant functional recovery and improved structural organization of the retina coinciding with the presence and distribution of retinoschisin in the treated eyes. Most notably, and in contrast to the untreated eye, the treated retina revealed an almost normal organization of the INL and ONL and an absence of gaps between bipolar cells.[16,18] There was also increased thickness of the ONL as a consequence of enhanced photoreceptor survival and a remarkable improvement in the structural integrity of the outer plexiform layer and INLs. A similar functional and structural rescue was found by Zeng *et al.*,[17] and in a recent follow-up by Kjellstrom *et al.*,[19] who evaluated AAV2-CMV-*Rs1h* treatment efficacy at 14 months after a single vector injection of the murine *Rs1h* gene at P14. This study also provided evidence for long-term rescue of rod outer and inner segments, reduced photoreceptor cell death, and relative preservation of ERG responses.

In this study, we aimed to systematically explore the effects of a single subretinal AAV5-mOPs-*RS1* injection into the retinoschisin-deficient ($Rs1h^{-/-}$) mouse retina at various stages of disease progression. In the context of a potential AAV-mediated gene replacement therapy option for humans with the disease, this issue assumes immediate importance, because the majority of patients may already have various degrees of disease pathology at the time they first present for treatment.

RESULTS

Time course of RS1 protein expression after subretinal injection of AAV5-mOP-*RS1*

As shown earlier, delivery of AAV5-mOP-*RS1* to the subretinal space in *Rs1h*-deficient mice resulted in a time lag before an improvement in the ERG b-wave amplitude was found.[16] The ERG showed no improvement in the b-wave amplitude 1 month after the injection, while a modest increase in the b-wave amplitude was observed at PM2. Three months after the injection, a significant increase in b-wave and a small but significant increase in the a-wave were observed. In order to determine whether retinoschisin expression and localization correlate with this delay in functional recovery, we examined retinal cryosections for retinoschisin at various time-points from 1 week to 12 weeks after subretinal injection of vector into 15-day-old retinoschisin-deficient mice. The typical pattern of protein expression is shown in **Figure 1**. No RS1 expression was observed 1 week after injection and only a few sporadically distributed photoreceptors were positive for retinoschisin at 2 weeks after injection. The number of labeled photoreceptors increased between the time-points of 3 weeks and 8 weeks after injection, and by 12 weeks almost all the photoreceptors across the retina were intensely labeled. Labeling of retinoschisin also increased along the longitudinal axis of the retina (**Figure 1**). At 2 weeks after injection, RS1 labeling was restricted to the inner segments of the photoreceptors. At 3 and 4 weeks after injection, RS1 labeling had spread to the ONL, with weak labeling observed in the outer plexiform layer. At 8 and 12 weeks after injection, more intense labeling was observed in the outer plexiform layer, with labeling observed to extend into the INL. This pattern of labeling is consistent with the expression and secretion of RS1 originating from the inner segments of photoreceptor cells and spreading to the other retinal layers. As the external surface of the inner segment becomes saturated with retinoschisin, the external surfaces of the photoreceptors' ONLs and outer plexiform layers become labeled. In this manner, over time, retinoschisin makes its way into the inner retina where it binds to the surface of the retinal bipolar cells, as observed earlier in the retinas of wild-type mice.[8,16] Recent studies indicate that RS1 binding to the surface of photoreceptor and bipolar cells is mediated through its interaction with Na/K ATPase.[20]

The finding that retinoschisin labeling is present in the outer plexiform layer at 8 and 12 weeks after injection is consistent with the improvement in ERG b-wave amplitudes observed at these time-points.

Time course of photoreceptor degeneration in the retinoschisin-deficient mouse

We have shown earlier that photoreceptor cell death in the *Rs1h*-deficient mouse is triggered by apoptotic events initiating at around P14 (refs. 21, 22). Histologically, this becomes evident in a progressive reduction in ONL thickness over time.[18,19] In order to further refine the time course and quantify the loss of photoreceptor cells in the *Rs1h*-deficient retina, we determined the number of cones and layers of the photoreceptor nuclei in the ONL over a 10-month period of disease progression (**Figure 2**). These values were compared to age-matched wild-type mice at three time-points from 15 days after birth to 13 months of age. Retinoschisin-deficient mice were analyzed at PM0.5, PM1, PM4, PM5, PM6, and PM10. At PM0.5 (15 days after birth), shortly before the major burst of apoptotic photoreceptor cell death occurs around P18 (18 days after birth) (refs. 21, 22), the photoreceptor nuclei count in *Rs1h*-deficient mice is almost identical to that in wild-type animals (94.1 ± 8.3; $P = 0.08$). In addition, as in age-matched wild-type controls, the knockout animals reveal ~500 cones per retinal section (**Figure 2** and data not shown). The further course of cell loss in the diseased retina follows a two-phase pattern, with an initially dramatic decrease of photoreceptors (>40%) within the first month of age. Thereafter, photoreceptor cell loss appears to slow and adopts a linear progression, with an average rate of cell death of 9.3 ± 2.0% ($P < 0.001$) per month. At 10 months of age, ~84% of the photoreceptors are lost in the diseased retina.

Subretinal AAV5-mOPs-*RS1* injections at various stages of disease progression

ERG responses. As shown earlier, ERG b-wave amplitudes are well suited for assessing the beneficial effects of AAV-mediated gene replacement therapy in retinoschisin-deficient mice.[16,19] Four groups of mice, given a single unilateral subretinal injection at PM0.5 (three males and two females), PM1 (two males and five females), PM2 (five females), and PM7 (four males), respectively,

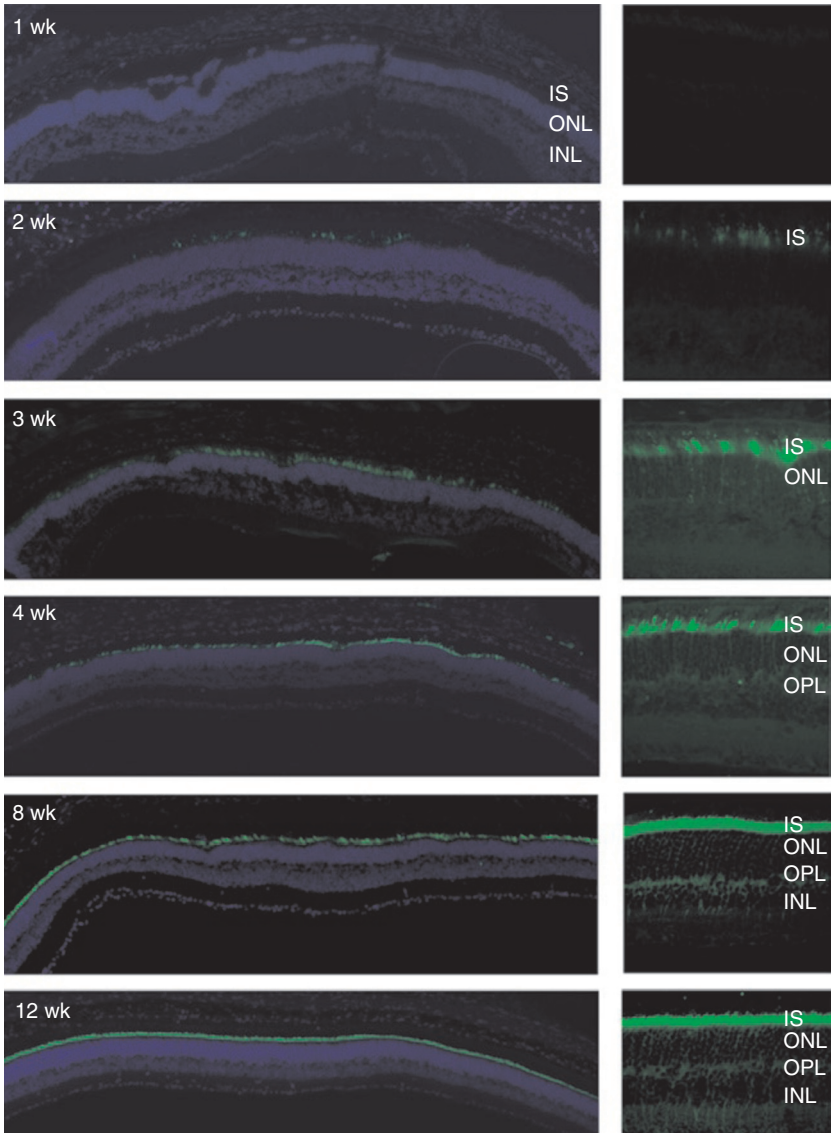

Figure 1 Immunofluorescence labeling of RS1 in retinal sections of Rs1h-deficient mice at various times after AAV5-mOP-*RS1* treatment. Subretinal injections were carried out on 15-day-old retinoschisin-deficient mice. Retinal cryosections at the indicated postinjection time-points were labeled with an anti-RS1 antibody and goat anti-rabbit immunoglobulin-tagged with Cy3 (green) and counterstained with 4′,6-diamidino-2-phenylindol nuclear (blue) dye to define the nuclear layers. Left: low-magnification image of the retina showing lateral distribution of label as a function of postinjection time-points; right: higher-magnification image of more densely stained regions of the retina showing longitudinal distribution of RS1 staining in the retinal layers. INL, inner nuclear layer; IS, inner segment; ONL, outer nuclear layer; OPL, outer plexiform layer.

were included in the ERG analysis (**Supplementary Table S1**). The time period between treatment and the recording of ERGs was maintained at 4 months. That is, ERGs were recorded at PM4.5 (group 1), PM5 (group 2), PM6 (group 3), and PM11 (group 4). A prominent increase in b-wave amplitude was observed in the treated eye relative to the untreated eye in mice that had been treated at 15 days after birth (**Figure 3a**). This is in full agreement with our earlier data.[16] An injection at PM1 still had a substantial positive effect 4 months later (**Figure 3b**), and a minor improvement was recordable in the group treated at PM2 (**Figure 3c**). Treatment at 7 months of age resulted in poor responses in retinal function when analyzed at 11 months after birth, with results similar to those in the untreated control eyes (**Figure 3d**). In order to assess potential differences between rod- and cone-system responses, we additionally recorded ERGs under photopic conditions. The positive effect on the cone system was approximately proportional to that on the rod system (lower pair of curves in **Figure 3a–d**). Statistical evaluation of the data reveals significant results for both scotopic and photopic recordings at PM0.5, PM1, and PM2 (**Figure 3e** and **f**). This suggests either a direct benefit of the treatment on cone survival and functionality or, alternatively, an indirect effect mediated through rod persistence, given that cone survival depends on rod integrity. The morphological status of rod and cone cells was then studied histologically for each treatment group.

Histology and immunohistochemistry. Animals included in the ERG study were killed at PM4.5 (group 1), PM9 (group 2), PM10

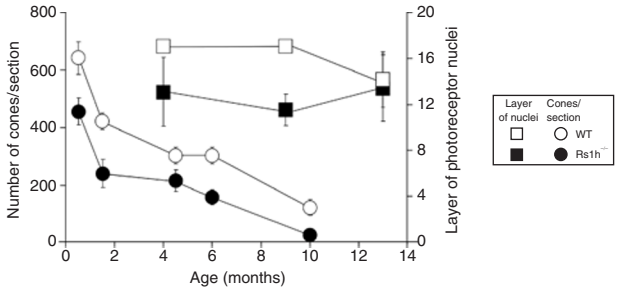

Figure 2 Evaluation of the extent of photoreceptor degeneration in retinal sections of Rs1h-deficient mice at various times after birth. Retinal cryosections of retinoschisin-deficient and wild-type (WT) mice were analyzed at the postnatal time-points indicated for the presence of cones (labeling with Alexa488 green-conjugated peanut agglutinin) (left *y*-axis) and photoreceptor nuclei (labeling with 4′,6-diamidino-2-phenylindol nuclear blue dye) (right *y*-axis). For each age group of animals, at least four eyes and three sections from each eye were included in the analysis. Bars represent mean number of cones (circles) and layers of photoreceptor nuclei (squares) ± SEM.

(group 3), and PM15 (group 4), and assessed for RS1 expression and tissue distribution by labeling retinal cryosections with polyclonal antibody RS1-3R10 (**Figure 4a–d**). As expected, untreated eyes remained unstained, demonstrating that RS1 protein is absent throughout the retina; the untreated eyes served as internal controls for natural disease progression. In contrast, RS1-specific labeling was present in AAV5-mOP-*RS1*-treated retinas from all four groups of mice. Eyes injected at PM0.5 (group 1) showed strong expression and a pattern of protein distribution nearly identical to that found in wild-type mice (**Figure 4a**). The eyes from the vector-treated as well as the age-matched wild-type mice revealed intense RS1 staining of photoreceptor inner segments and weaker labeling of the ONL and outer plexiform layer. There was also distinct immunostaining of the outer membranes of the retinal bipolar cells and labeling of the inner plexiform layer. These findings are fully consistent with the data from our earlier study.[16] Eyes injected at PM1 (**Figure 4b**), PM2 (**Figure 4c**), and PM7 (**Figure 4d**) still showed strong RS1 labeling at the level of the photoreceptor inner segments, but exhibited attenuated ONL thickness and disturbances in retinal structure well correlated with the stage of disease progression at the time of treatment. RS1 labeling of retinal bipolar cells and the inner plexiform layer after treatment at PM1 and PM2 is similar to that in the retinas of wild-type animals but decreases markedly in retinas treated at PM7.

Photoreceptor survival in AAV5-mOPs-*RS1*-treated versus untreated eyes was quantified by two measures. First, by fluorescence-conjugated peanut agglutinin which specifically labels cone photoreceptors and photoreceptor-bipolar synaptic regions; and second, by 4′,6-diamidino-2-phenylindol nuclear dye staining which identifies both cone and rod photoreceptor nuclei in the ONL (**Figure 4a–d**). In untreated eyes, the number of cones as well as the number of layers of photoreceptor nuclei follow a linear decrease with an average of 131.6 ± 40.3 cones/section (6.0 ± 0.5 rows of nuclei/section) for group 1 animals (27 retinal sections analyzed) and 34.8 ± 23.2 cones/section (2.5 ± 0.6 rows of nuclei/section) for group 4 mice (21 retinal sections analyzed) (**Figure 5a** and **b**, **Table 1**). This leads to a calculated rate of loss of photoreceptor cells of ~10.2% per month, in good agreement with the rates established for the general course of disease progression (**Figure 2**). For vector-treated eyes, both the loss of cones ($P \leq 2.3 \times 10^{-8}$) as well as the overall loss of rows of photoreceptor nuclei ($P \leq 8.5 \times 10^{-4}$) were significantly less pronounced as in partner untreated eyes in each of the four groups analyzed (**Figure 5a** and **b**). On average, there was a (2.7 ± 0.5)-fold higher cone count and a (1.9 ± 0.4)-fold increase in the rows of photoreceptor nuclei in treated versus untreated eyes following each time-point of injection.

Taken together, morphological changes in untreated eyes closely followed the known course of retinal degeneration in retinoschisin-deficient mice, as described earlier.[18,19] Most notably, all the age groups that were studied showed a significant loss of photoreceptor cells, in particular cones, closely accompanied by an almost complete loss of peanut agglutinin–labeling of ribbon synapsis (**Figure 4a–d**). Retinas treated at progressively later time-points of disease progression showed progressively less preservation. However, whatever the time-point at which the treatment was given, the rate and extent of degeneration in the treated eye were significantly less pronounced at the time of evaluation than in the untreated control eye of the same animal (**Figures 4** and **5**). At PM1 and PM2, and even in the most advanced age group (PM7), AAV5-mOPs-*RS1*-injected eyes still retained a retinal architecture that represented a marked improvement over the control eyes, as determined on the basis of (i) preservation of photoreceptor cells, including cones; (ii) the presence of photoreceptor-bipolar synaptic ribbons; (iii) thinned but preserved ONL and INL; and (iv) histologically distinct inner and outer plexiform layers (**Figure 4a–d**).

DISCUSSION

In this study, we explored the efficacy of AAV-mediated gene replacement in a well-established mouse model of XLRS as a function of the stage of the disease. We show that a significant functional benefit of therapy (in terms of ERG responses) is detectable even in mice that received treatment only as late as 2 months after birth. This functional recovery is reflected in the preservation of retinal architecture in the treated eyes as compared to the untreated ones, and by the presence of a retinal distribution of expressed retinoschisin that is remarkably similar to that seen in retinas of wild-type mice. Most notably, photoreceptor cell preservation is 2.3-fold higher in treated eyes in comparison with untreated eyes, independent of the time-point (after birth) at which vector treatment was administered. This is consistent with findings in an independent study, where retinoschisin-deficient mice were treated with AAV 2-CMV-Rs1h as late as PM3.[17] Although retinoschisin replacement at this late time-point of initiation of treatment did not result in repair of the retinal structure, it was nevertheless successful in reversing the functional abnormality of the b-wave. Together, these findings bode well for future gene therapy trials in humans, as they suggest that AAV-mediated delivery of retinoschisin into the diseased retina might be beneficial to patients even when treatment is administered at a relatively advanced disease stage.

An analysis of the documented time course of RS1 expression after subretinal injection of AAV5-mOP-*RS1* in retinoschisin-deficient mice demonstrated that there is a delay of as much as

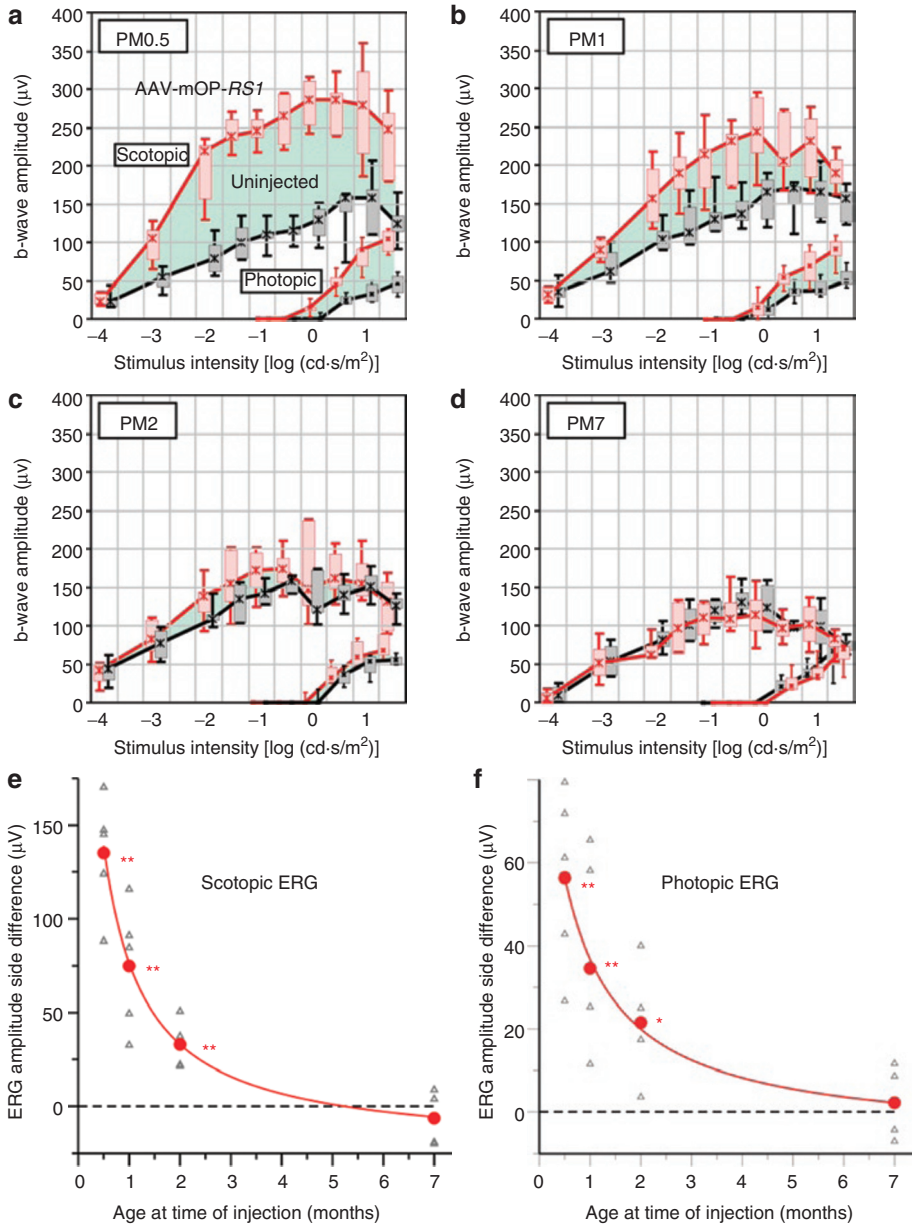

Figure 3 Electroretinogram (ERG) evaluation of AAV5-mOP-*RS1* injections as a function of age at the time of treatment. (**a–d**) Electrophysiological evaluation of AAV-mOPs-*RS1*-treated and untreated control eyes from retinoschisin-deficient mice injected at (**a**) PM0.5, (**b**) PM1, (**c**) PM2, and (**d**) PM7, each analyzed 4 months after treatment. For each time-point of injection, dark-adapted (scotopic) and light-adapted (photopic) single-flash ERG b-wave amplitudes were recorded from treated eyes (red) and untreated eyes (black) of the same mouse as a function of the logarithm of the flash intensity. Boxes indicate the 25–75% quantile range, whiskers indicate the 5 and 95% quantiles, and the asterisks indicate the median of the data. The green shading between treated eye and untreated eye medians indicates the functional benefit of treated eye over untreated eye in terms of ERG b-wave amplitude gain. (**e** and **f**) Statistical evaluation of (**e**) scotopic and (**f**) photopic ERG b-wave amplitude side differences for the time-points shown in **a–d**. Each open triangle represents data from an individual mouse (see Materials and Methods for details), dots indicate the mean values across mice, and the line is a hyperbolic fit. Asterisks show the level of significance of the differences; $*P < 0.05$, $**P < 0.01$.

2 months after the injection before protein distribution within the retina mimics the wild-type pattern. That is, the full rescue effect of vector treatment is realized only after functional retinoschisin is available at all retinal structures in which it is normally found. Given that RS1 expression takes place primarily in photoreceptors and then must be secreted and localized to its correct positions throughout the retina, it may not be surprising that protein distribution is delayed quite significantly relative to its simple expression in the photoreceptors. Considering that almost 40% of retinoschisin-deficient photoreceptor cells die within the first month of birth, followed by a further loss of cones and rods at a rate of ~10% per month, we conclude that even early treatment (at postnatal day 15 or PM1) may have to face the challenge of a retinal environment already suffering substantial (perhaps 50%) loss of photoreceptors. In this context, it is extraordinary that the rescue seen at the first two time-points of injection is so robust (ref. 16 and this study), and suggests that photoreceptors display tremendous plasticity in response to retinoschisin treatment. Even more surprising is the

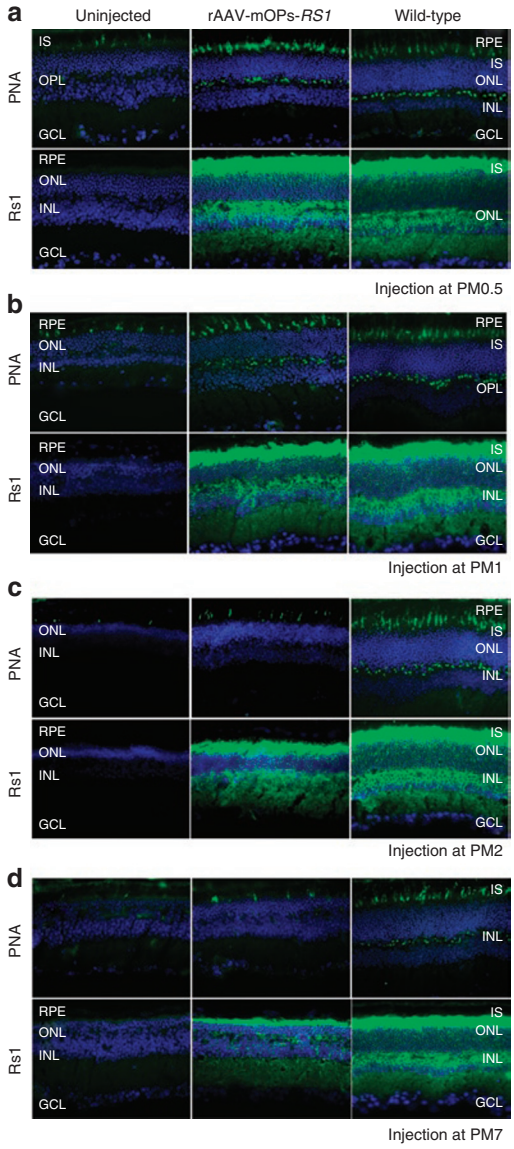

Figure 4 Immunofluorescence labeling of RS1 and Alexa488-conjugated peanut agglutinin (PNA) in retinal sections of wild-type, treated, and untreated eyes of Rs1h-deficient mice at various time-points after AAV-mOP-*RS1* injections. Subretinal injections were administered in retinoschisin-deficient mice at (**a**) PM0.5, (**b**) PM1, (**c**) PM2, and (**d**) PM7, while retinal cryosections were analyzed at the ages of (**a**) 4 months and (**b**–**d**) 8 months after injection. Labeling was done using Alexa488 (green)-conjugated PNA so as to specifically stain cone inner segments and photoreceptor-bipolar synaptic regions. For labeling of photoreceptor inner segments, RS1-3R10 (RS1) antibody and anti-rabbit immunoglobulin-tagged with Alexa488 (green) were used. Retinal sections were counterstained with 4′,6-diamidino-2-phenylindol nuclear dye (blue) to define the nuclear layers. Data relating to untreated eye (left column) and treated eye (middle column) refer to the same individual mouse in each case. Data from age-matched control mice are shown for comparison on the right. GCL, ganglion cell layer; INL, inner nuclear layer; IS, inner segment; ONL, outer nuclear layer; OPL, outer plexiform layer; RPE, retinal pigment epithelium.

vector-mediated retinal rescue seen after treatment at PM2, even though there would have been substantial photoreceptor loss, inner segment shortening of the remaining photoreceptors, and retinal disorganization at this time-point. This suggests that retinoschisin

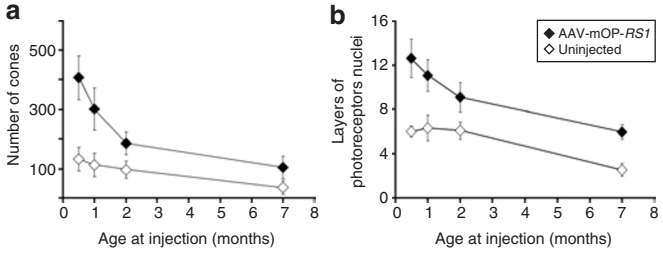

Figure 5 Evaluation of photoreceptor cell rescue in AAV5-mOP-*RS1*-treated versus untreated retinas of retinoschisin-deficient mice, in relation to the time-points at which treatment was administered. (**a**) The total number of cones per retinal section was counted after staining with Alexa488 (green)-conjugated peanut agglutinin. (**b**) Likewise, the number of rows of photoreceptor nuclei was determined per retinal section after 4′,6-diamidino-2-phenylindol nuclear dye (blue) staining. Bars represent the mean number of cones (**a**) and layers of photoreceptor nuclei (**b**) of Rs1h-deficient treated (filled symbols) and untreated (unfilled symbols) retinas. Three retinal sections were evaluated for each of the eyes analyzed (**Table 1**). *P* values for AAV-mOP-*RS1*-treated and untreated eyes were calculated using the paired Student's *t*-test ($*P \leq 8.5 \times 10^{-4}$; $**P \leq 2.3 \times 10^{-8}$).

protein may be capable of rescuing diseased photoreceptors from apoptotic cell death, although retinoschisin alone does not appear capable of effecting a complete repair of all morphological retinal cell damage that predated the treatment.

ERG responses and the level of rescue of the retinal structure appear discordant at some time-points, with the beneficial effects of treatment on retinal structure being more evident than those on function at time-point PM2 and, to some extent, even at PM7. This may be because of progressive deterioration of functionally essential structures such as synapses, gap junctions, and cone pedicles, which may not be reversible by later treatment. Impairment of substructural elements may lead to "retired" cells that are morphologically still present but do not contribute further to function. Alternatively, Ganzfeld ERG responses for treatment at advanced disease stages could fall below a recordable threshold although areas of functionality may still exist. In order to address this possibility, an improved resolution of multifocal ERG recordings may be required. Importantly, our findings emphasize the need for both functional and morphological follow-up approaches in therapy assessment studies.

In summary, this study builds on previous demonstrations of proof-of-concept of gene therapy in independent mouse models for XLRS. It delineates the window of rescue, in terms of disease duration at the time of vector injection. Accordingly, gene replacement therapy at an early stage of the disease can effectively restore visual function, and there is a gradual decline in the rescue effect when treatment is administered at more advanced stages of the disease. This study demonstrates that, even when treatment is initiated only at an advanced stage of the disease, RS1 gene replacement therapy may be successful in slowing disease progression and averting further photoreceptor cell death.

MATERIALS AND METHODS

Mice. The method of generation and the phenotypic characterization of the *Rs1h*-knockout mouse line used in this study have been reported earlier.[18] The line has been backcrossed for more than 10 generations onto a pure C57BL/6 background. A total of 33 *Rs1h*-deficient mice were injected with AAV5-mOP500-hRS1 at various time-points after birth: nine

Table 1 Quantitative measure of photoreceptor loss in AAV5-mOPs-*RS1*-treated and untreated retinae

		Untreated retina[a]		AAV5-mOPs-*RS1*-treated retina[a]	
Age at injection (month)	No. of mice analyzed	No. of cones per section (±SD)	No. of rows of photoreceptor nuclei (±SD)	No. of cones per section (±SD)	No. of rows of photoreceptor nuclei (±SD)
0.5	9	131.6 ± 40.3	6.0 ± 0.5	407.0 ± 74.0	12.6 ± 1.7
1	10	111.5 ± 40.0	6.3 ± 1.2	300.9 ± 71.1	11.1 ± 1.4
2	7	95.1 ± 28.8	6.1 ± 0.8	184.7 ± 38.0	9.1 ± 1.3
7	7	34.8 ± 23.2	2.5 ± 0.6	102.8 ± 38.0	5.9 ± 0.7

[a]Three retinal sections per eye were analyzed, respectively.

animals (four males and five females) at day 15 (PM0.5), ten (three males and seven females) at 1 month (PM1), seven (one male and six females) at 2 months (PM2), and seven (six males and one female) at 7 months (PM7). The animals were reared under standard laboratory conditions (22 ± 2 °C, 60 ± 10% relative humidity, and a 12-hour light–dark cycle) and had free access to food and water throughout the experiment. The conditions of housing and experiments were in accordance with the Association for Research in Vision and Ophthalmology Statement for the Use of Animals in Ophthalmic and Vision Research, and with the protocols approved by the University of Florida Institutional Animal Care and Use Committee and the Animal Care and Use Committee of the University of Regensburg.

Time course of AAV5-mOP500-hRS1 expression. The right eye of each of 35 *Rs1h*-deficient mice was injected with AAV5-mOP500-hRS1 at postnatal day 15. Seven mice were killed at 1 week, nine at 2 weeks, seven at 3 weeks, five at 4 weeks, three at 8 weeks, and four at 12 weeks after the injection. The eyes were enucleated and fixed with 4% paraformaldehyde in 0.1 mol/l phosphate buffer (PB) (pH 7.4) containing 5% sucrose for 1.5 hours and rinsed in PB containing 5% sucrose. The eyes were cryoprotected with 8, 12, 16, and 20% sucrose, in PB before being frozen in OCT. Cryosections were blocked and permeabilized in 10% normal goat serum and 0.2% Triton X-100 in PB for 30 minutes and subsequently labeled overnight with anti-RS1 polyclonal antibody diluted 1:3,000 in PB containing 2.5% normal goat serum and 0.1% Triton X-100. Sections were rinsed in PB and labeled for 1 hour with goat anti-rabbit immunoglobulin conjugated with Cy3 (Cedar Lane, Burlington, Canada). Labeled retinal sections were examined under a Zeiss Axioplan2 fluorescence microscope equipped with an Eclipse digital analyzer.

In order to study the course of photoreceptor degeneration after vector injection at defined time-points postnatally, nine hemizygous male knockout mice were killed at PM0.5, PM1.5, PM4.5, PM6, and PM10. Eleven C57BL/6 wild-type animals, purchased from Charles River (Sulzfeld, Germany), served as age-matched controls.

AAV5-mOP500-hRS1 construct and delivery. Generation and delivery of the AAV5 vector containing the human *RS1* cDNA under the control of the mouse opsin promoter (AAV5-mOPs-*hRS1*) has been described earlier.[16] Briefly, the full-length human *RS1* was cloned into the pTR-AAV plasmid containing AAV-inverted terminal repeats and a proximal mouse opsin promoter (mOP-500) which restricts expression to photoreceptors. This serotype 2 vector DNA then packaged into serotype 5 capsids resulting in a pseudotyped vector, sometimes referred to as AAV2/5, but referred to here simply as AAV5. The titers of the vectors were adjusted to 4×10^{13} vector genomes/ml. Before the injection, the animals were anesthetized with IP ketamine (66.7 mg/kg) and xylazine (11.7 mg/kg), and the right eye of each mouse was dilated with 1% atropine sulfate and 2.5% phenylephrine hydrochloride. After the application of 2.5% hydroxypropyl methylcellulose (Eye Supply USA, Tampa, FL), the cornea was punctured carefully with a 30G1/2 gauge needle guided by an operating microscope so as to avoid lens damage. A blunt 33-gauge needle (Hamilton, Reno, NV) was then inserted through the corneal hole, maneuvered around the lens, displacing it medially, and was directed toward the subretinal space of the inferior hemisphere. A total of 1 µl volume of vector with fluorescein tracer (0.1 mg/ml) was used for each injection. An antibiotic (Vetropolycin, Pharmaderm, NY) was applied daily to the cornea for 3 days following the procedure. The other (left) eye of each treated animal was left untouched and served as internal control.

Electroretinography. ERGs were performed according to procedures described earlier.[23] The ERG equipment consisted of a Ganzfeld bowl, a direct-current amplifier, and a personal computer–based control and recording unit (Multiliner Vision; Viasys Healthcare, Hoechberg, Germany). The mice were dark-adapted overnight and anesthetized using ketamine (66.7 mg/kg) and xylazine (11.7 mg/kg). The pupils were dilated, and single-flash ERG recordings were obtained under dark-adapted (scotopic) and light-adapted (photopic) conditions. Light adaptation was accomplished with a background illumination of 30 cd/m^2 starting 10 minutes before recording. Single white-flash stimulation ranged from 10^{-4} to 25 cd·s/m^2, divided into 10 steps of 0.5 and 1 log cd·s/m^2. Ten responses were averaged with an interstimulus interval of either 5 seconds or 17 seconds (for 1, 3, 10, and 25 cd·s/m^2). A statistical evaluation of the ERG data was performed. First, b-wave amplitude differences between the treated and the untreated eyes were obtained for each animal at each intensity value of the stimulus supplied. For scotopic recordings, the median of these data across intensities from 10^{-2} to 25 cd·s/m^2 was determined for each mouse. For photopic recordings, only the difference at 25 cd·s/m^2 was used for each mouse. As saturation was not reached, this intensity yields the largest difference under the given conditions. These data are shown in **Figure 3e** and **f** as open triangles. A paired *t*-test was used for determining the level of significance of the differences between the treated and the untreated eyes across mice, separately for each time-point of vector injection.

Histology and immunohistochemistry. The eye bulbs of treated and untreated eyes were removed and embedded in O.T.C. compound without fixation, with care being taken to hold the eyes in a standardized position (Tissue Tek; Sakura Finetek, Zoeterwoude, The Netherlands). In order to ensure that all retinal sections were derived from the same position of the central inner retina at the level of the anatomical midline of the eye, sections were cut sagittally on a cryostat (10 µm). The outline of the lens served as orientation. Mice injected at PM0.5 were analyzed 4 months after injection, while animals injected at PM1, PM2, and PM7 were killed for analysis 8 months after injection. Three retinal sections each from the injected right eye and the noninjected left eye of each animal were analyzed. For each retinal section, the total number of cones and layers of photoreceptor nuclei was counted along the longitudinal axis of the entire retina. The results were combined groupwise, and 27 (group 1), 30 (group 2), 21 (group 3), and 21 (group 4) retinal sections were included in the statistical evaluation. The sections were postfixed in 4% paraformaldehyde at room temperature for 6 minutes and rinsed several times in phosphate buffered saline. The sections were then blocked (1% dry milk; 0.1% Tween 20 in phosphate-buffered saline) for 30 min at room temperature. Subsequently, the sections were stained with monoclonal antibody RS1-3R10 (1:250) specific to human retinoschisin,[9] and with peanut agglutinin (1:800) specific to cone photoreceptor inner segments, in 2%

bovine serum albumin, 0.02% sodium azide, and 0.1% Triton X-100 in phosphate-buffered saline. Sections stained for RS1-3R10 were incubated with Alexa-conjugated secondary antibodies (1:1,000; Molecular Probes, Leiden, The Netherlands). The sections were counterstained with 4′,6-diamidino-2-phenylindol (Molecular Probes, Leiden, The Netherlands). The slides were mounted in Fluorescent Mounting Medium (Dako Cytomation, Glostrup, Denmark) and analyzed using an Axioskop 2 (Carl Zeiss, Oberkochen, Germany).

ACKNOWLEDGMENTS

This work was supported in part by grants from Macula Vision Research Foundation (to B.H.F.W., R.M., and W.W.H.), Foundation Fighting Blindness (to B.H.F.W., R.M., and W.W.H.), National Institutes of Health EY11123 (to W.W.H.), EY02422 (to R.M.), NS36302 (to W.W.H.), EY13729 (to W.W.H.), EY08571 (to W.W.H.), Research to Prevent Blindness (to W.W.H.), German Research Council DFG Se837/4-1 and 5-1 (to M.W.S.), and a European Community Grant IP "EVI-GenoRet" LSHG-CT-512036 (to M.W.S.). None of the authors declares a financial conflict of interest.

SUPPLEMENTARY MATERIAL

Table S1. Characteristics of individual mice analyzed in the present study.

REFERENCES

1. Haas, J (1898). Ueber das Zusammenvorkommen von Veraenderungen der Retina und Choroidea. *Arch Augenheilkd* **37**: 343–348.
2. George, ND, Yates, JR and Moore, AT (1995). X linked retinoschisis. *Br J Ophthalmol* **79**: 697–702.
3. Kellner, U, Brummer, S, Foerster, MH and Wessing, A (1990). X-linked congenital retinoschisis. *Graefes Arch Clin Exp Ophthalmol* **228**: 432–437.
4. Roesch, MT, Ewing, CC, Gibson, AE and Weber, BH (1998). The natural history of X-linked retinoschisis. *Can J Ophthalmol* **33**: 149–158.
5. Khan, NW, Janison, JA, Kemp, JA and Sieving, PA (2001). Analysis of photoreceptor function and inner retinal activity in juvenile X-linked retinoschisis. *Vision Res* **41**: 3931–3942.
6. Sauer, CG, Gehrig, A, Warnecke-Wittstock, R, Marquardt, A, Ewing, CC, Gibson, A *et al.* (1997). Positional cloning of the gene associated with X-linked juvenile retinoschisis. *Nat Genet* **17**: 164–170.
7. Grayson, C, Reid, SN, Ellis, JA, Rutherford, A, Sowden, JC, Yates, JRW *et al.* (2000). Retinooschisin, the X-linked retinoschisin protein, is a secreted photoreceptor protein, and is expressed and released by Weri-Rb1 cells. *Hum Mol Genet* **9**: 1873–1879.
8. Molday, LL, Hicks, D, Sauer, CG, Weber, BH and Molday, RS (2001). Expression of X-linked retinoschisis protein RS1 in photoreceptor and bipolar cells. *Invest Ophthalmol Vis Sci* **42**: 816–825.
9. Wu, WW and Molday, RS (2003). Defective discoidin domain structure, subunit assembly, and endoplasmatic reticulum processing of retinoschisin are primary mechanisms responsible for X-linked retinoschisis. *J Biol Chem* **278**: 28139–28146.
10. Reid, SN and Farber, DB (2005). Glial transcytosis of a photoreceptor-secreted signaling protein, retinoschisin. *Glia* **49**: 397–406.
11. Wu, WW, Wong, JP, Kast, J and Molday, RS (2005). RS1, a discoidin domain-containing retinal cell adhesion protein associated with X-linked retinoschisis, exists as a novel disulfide-linked octamer. *J Biol Chem* **280**: 10721–1030.
12. Simpson, DL, Rosen, SD and Barondes, SH (1974). Discoidin, a developmentally regulated carbohydrate-binding protein from *Dictyostelium discoideum*. Purification and characterization. *Biochemistry* **13**: 3487–3493.
13. Baumgartner, S, Hofmann, K, Chiquet-Ehrismann, R and Bucher, P (1998). The discoidin domain family revisited: new members from prokaryotes and a homology-based fold prediction. *Protein Sci* **7**: 1626–1631.
14. Vogel, W (1999). Discoidin domain receptors: structural relations and functional implications. *FASEB J* **13**: 77–82.
15. Wang, T, Zhou, A, Waters, CT, O'Connor, E, Read, RJ and Trump, D (2006). Molecular pathology of X linked retinoschisis: mutations interfere with retinoschisin secretion and oligomerisation. *Br J Ophthalmol* **90**: 81–86.
16. Min, SH, Molday, LL, Seeliger, MW, Dinculescu, A, Timmers, AM, Janssen, A *et al.* (2005). Prolonged recovery of retinal structure/function after gene therapy in an Rs1h-deficient mouse model of x-linked juvenile retinoschisis. *Mol Ther* **2**: 644–651.
17. Zeng, Y, Takada, Y, Kjellstrom, S, Hiriyanna, K, Tanikawa, A, Wawrousek, E *et al.* (2004). RS-1 gene delivery to an adult Rs1h knockout mouse model restores ERG b-wave with reversal of the electronegative waveform of X-linked retinoschisis. *Invest Ophthalmol Vis Sci* **45**: 3279–3285.
18. Weber, BH, Schrewe, H, Molday, LL, Gehrig, A, White, KL, Seeliger, MW *et al.* (2002). Inactivation of the murine X-linked juvenile retinoschisis gene, Rs1h, suggests a role of retinoschisin in retinal cell layer organization and synaptic structure. *Proc Natl Acad Sci USA* **99**: 6222–6227.
19. Kjellstrom, S, Bush, RA, Zeng, Y, Takada, Y and Sieving, PA (2007). Retinoschisin gene therapy and natural history in the Rs1h-KO mouse: long-term rescue from retinal degeneration. *Invest Ophthalmol Vis Sci* **48**: 3837–3845.
20. Molday, LL, Wu, WW and Molday, RS (2007). Retinoschisin (RS1), the protein encoded by the X-linked retinoschisis gene, is anchored to the surface of retinal photoreceptor and bipolar cells through its interactions with a Na/K ATPase-SARM1 complex. *J Biol Chem* **282**: 32792–32801.
21. Gehrig, A, Janssen, A, Horling, F, Grimm, C and Weber, BH (2006). The role of caspases in photoreceptor cell death of retinoschisin-deficient mouse. *Cytogenet Genome Res* **115**: 35–44.
22. Gehrig, A, Langmann, T, Horling, F, Janssen, A, Bonin, M, Walter, M *et al.* (2007) Genome-wide expression profiling of the retinoschisin-deficient retina in early postnatal mouse development. *Invest Ophthalmol Vis Sci* **48**: 891–900.
23. Seeliger, MW, Grimm, C, Stahlberg, F, Friedburg, C, Jaissle, G, Zrenner, E *et al.* (2001). New views on RPE65 deficiency: the rod system is the source of vision in a mouse model of Leber congenital amaurosis. *Nat Genet* **29**: 70–74.